The 15th International Symposium on Magnetic Bearings, August 3-6, 2016, Mojiko Hotel, Kitakyushu, Japan

ISMB15

Design of Robust AMB Controllers for Rotors Subjected to Varying and Uncertain Seal Forces

Jonas LAURIDSEN* and Ilmar SANTOS*

* Dept. of Mechanical Eng., Technical University of Denmark
Copenhagen, Denmark
E-mail: ifs@mek.dtu.dk

Abstract

This paper demonstrates the design and simulation results of model based controllers for AMB systems, subjected to uncertain and changing dynamic seal forces. Specifically, a turbocharger with a hole-pattern seal mounted across the balance piston is considered. The dynamic forces of the seal, which are dependent on the operational conditions, have a significant effect on the overall system dynamics. Furthermore, these forces are considered uncertain. The nominal and the uncertainty representation of the seal model are established using results from conventional modelling approaches, i.e. CFD and Bulkflow, and experimental results. Three controllers are synthesized: I) An $\mathcal{H}_\infty$ controller based on nominal plant representation, II) A μ controller, designed to be robust against uncertainties in the dynamic seal model and III) a Linear Parameter Varying (LPV) controller, designed to provide a unified performance over a large operational speed range using the operational speed as the scheduling parameter.

Key words : Uncertain dynamic seal forces, Robust control, LPV control, AMB, Turboexpander, Hole-pattern seal, Fluid interaction.

1. Introduction

Annular seals in rotordynamic systems can generate significant dynamic forces, and under certain conditions, destabilize the system leading a to machine failure. In rotordynamic systems supported by Active Magnetic Bearings (AMBs) these forces can, to a certain degree, be compensated for by employing appropriate feedback controllers. However, incorporating seal dynamics into the control design can be challenging due to, among other things, the frequency dependence of seal forces, varying operating conditions, process fluid characteristics and model uncertainties.

A number of publications have been presented focusing on the mathematical description of seal dynamics using either CFD or empirically-based Bulkflow models, and it has been shown that for seals under well defined single phase conditions a reasonable match between theoretical and experimental results can be achieved (Nielsen et al., 2012). However, seal dynamics under multiphase conditions, i.e. where the fluid is a mixture of gas and liquid, are still challenging. Larger model uncertainties should be expected for seals under multiphase conditions due to a limited knowledge of the dynamic behaviour of such fluids, especially when combined with complex seal geometries such as hole-pattern and labyrinth. Model uncertainties are thus inevitable due to these limitations of the mathematical models. Furthermore, seal model parameters change depending on operational conditions such as rotational speed and pressure difference across the seal.

Some research has focused on how fluid film forces can be compensated for by AMB systems aided by model-based control design (Lang et al., 1996; Mushi et al., 2008; Pesch & Sawicki, 2015). However, the main focus of this work has been on investigating the possibility for designing model based control to compensate and stabilize well known cross coupled stiffness effects under nominal conditions.

A large quantity of research has focused on designing robust control for AMB systems. (Balas & Young, 1995) shows that robust controllers for uncertain rotational speed can be addressed using a LFT consisting of the nominal system, a representation of how the system changes due to gyroscopic effects and a repeated uncertainty. In (Schonhoff et al., 2000) uncertainties of the natural frequencies of the flexible shaft's bending modes are considered and a robust controller is designed using μ synthesis. Robust stability to additive and multiplicative uncertainties can directly be ensured by applying complex weighting functions to the transfer functions CS (controller sensitivity) and T (complementary sensitivity). The conservativeness of the robust controller design can be reduced in the case of Linear Parameter Varying (LPV) controller

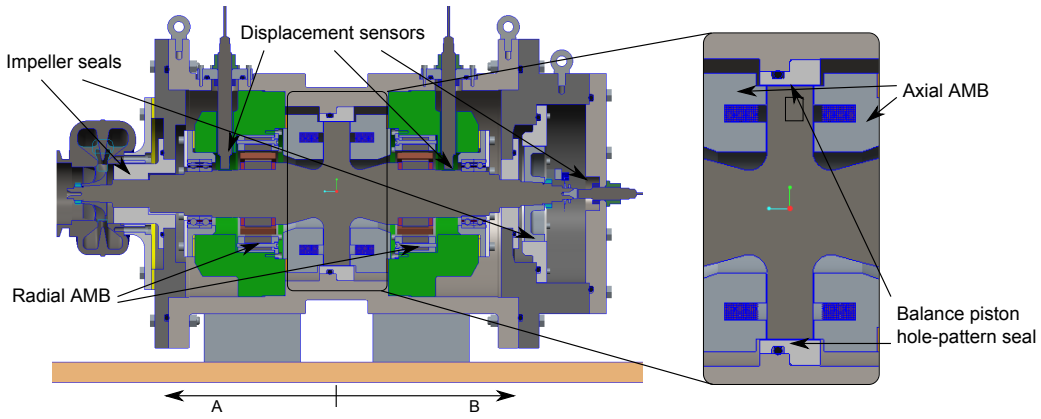

Fig. 1 Cross section of the turboexpander testrig. An enlargement of the center section section shows the balance piston on which the axial bearings acts and where the hole-pattern seal are placed

design, where one or more parameters are measured in real time, and can represent changing dynamics, which otherwise would be considered uncertain. A measured parameter could be the rotation speed, which can be utilized to reduced synchronous vibrations as shown in (Balini et al., 2012).

This paper presents a mathematical model of a high speed turboexpander unit used for cryogenic air separation and the design of model-based feedback controllers for the pair of radial AMBs responsible for magnetic levitation and stabilization. One hole-pattern seal is placed across a balance piston in the center of the turboexpander generating a thrust force to oppose the sum of the impeller thrust forces. The seal dynamics is considered uncertain and further changes due to operating conditions. A robust LTI controller is designed using μ synthesis to compensate for uncertain seal forces and is compared to an $\mathcal{H}_\infty$ controller based on the nominal model. For improved performance, an LPV controller is designed, which schedules controllers depending on the rotational speed. A performance comparison between the controllers based on the nominal model, the uncertain system representation and parameter varying model is presented.

2. Modelling of the Turboexpander

A cross-section schematic of the turboexpander investigated is shown in Fig. 1. The turboexpander essentially consists of a shaft levitated using axial and radial AMBs, and three annular seals. It is assumed that the only significant forces acting on the rigid rotor are the left and right side radial AMB and the seal in the center. The displacement sensors are placed close to the AMBs. The axial placement of the sensors and actuators are denoted by A and B, indicated in Fig. 1, with subscript x, y indicating the radial movement in the global horizontal and vertical coordinate system. The analysis will be focused on rotor lateral movements; for simplicity the rotor axial movements will not be investigated. The term AMB will therefore refer to the radial AMBs in the rest of this work.

2.1. AMB Model

The model of the magnetic bearing is simplified to describe the forces acting on the rotor as function of the rotor lateral displacements to AMB s_x and the control current i_x. The linearised expression of the forces are given as

$$f_b(i_x, s_x) = K_i i_x + K_s s_x \tag{1}$$

where K_i are K_s are constants. The dynamics of the electromechanical system, including the inductance of the coil and the amplifiers, is approximated as a first order system with a 3 dB cut-off frequency at 1.5 kHz, denoted G_{act}.

2.2. Model of Shaft

The rotating shaft is modelled using the Finite Element (FE) method and Bernoulli-Euler beam theory taking into account the gyroscopic effects of the shaft and discs (Nelson, 1980). The shaft model is discretized into 40 node points with 4 degrees of freedom each, i.e. x and y direction, and the rotation around the x and y axes, which yields 320 states in total. The full order rotordynamic system G_f consisting of the finite element model of the shaft and negative stiffness forces from the AMB can be written in state space form

$$\dot{x}_f = A_f x_f + B_f u, \quad y = C_f x_f \tag{2}$$

Using modal truncation techniques, real left and right modal transformation matrices are obtained which transform the full order FE system to a reduced form, shown in Eq. (3). The first bending mode of the shaft lies at approx. 1 kHz. Since this is substantially above the frequency range of interest in this work, the shafts is assumed rigid and all bending modes have thus been removed in the reduced order model. The FE model is selected though for generality and for possibility of to extend the model to included some of the bending modes if needed.

$$x = T_L{}^T x_f, \quad A = T_L{}^T A_f T_R, \quad B = T_L{}^T B_f, \quad C = C_f T_R \tag{3}$$

2.3. Seal Model - CFD vs Bulkflow

CFD and Bulkflow methods are typically used to obtain the static and dynamic properties of seals. CFD has been shown to be able to find seal forces even with complex geometries but can be extremely time demanding and computational heavy, since full 3D flow and pressure fields have to be calculated. On the other hand Bulkflow models are much simpler since these are based on simplified 1D models heavily linked to empirical parameters. The results of both CFD and Bulkflow modelling are usually validated against experimental data. Industrial software like ISOTSEAL is based on Bulkflow models and is widely used in the industry. Independent of the modelling approach, the dynamic seal forces are usually represented by their linearised force coefficients: stiffness, damping and sometimes mass matrices:

$$\begin{bmatrix} f_x \\ f_y \end{bmatrix} = \begin{bmatrix} K & k \\ -k & K \end{bmatrix} \begin{bmatrix} x \\ y \end{bmatrix} + \begin{bmatrix} C & c \\ -c & C \end{bmatrix} \begin{bmatrix} \dot{x} \\ \dot{y} \end{bmatrix} + \begin{bmatrix} M & 0 \\ 0 & M \end{bmatrix} \begin{bmatrix} \ddot{x} \\ \ddot{y} \end{bmatrix} \tag{4}$$

This model has a symmetric structure since the shaft is assumed to be approximately in the center. The sign difference of the cross coupled stiffness and damping coefficients is commonly known to cause instability. The coefficients are a function of the rotational speed and the excitation frequency. The seal used in the turboexpander application is a hole-pattern seal with coefficients taken from (Nielsen et al., 2012). The coefficients are given for a constant rotational speed of 20,200 RPM and with excitation frequencies varying from 20-300 Hz, and the specifications are stated in Fig. 2. The

Parameter	Value
Seal Length [mm]	85.70
Rotor Diameter [mm]	114.74
Inlet Clearance [mm]	0.2115
Exit Clearance [mm]	0.2102
Hole Depth [mm]	3.30
Hole Diameter [mm]	3.18
Hole Area Ratio	0.684
Rotor Speed [rpm]	20200
Inlet Pressure [bar]	70.0
Outlet Pressure [bar]	31.5
Res. Temperature [C]	17.4
Preswirl	0

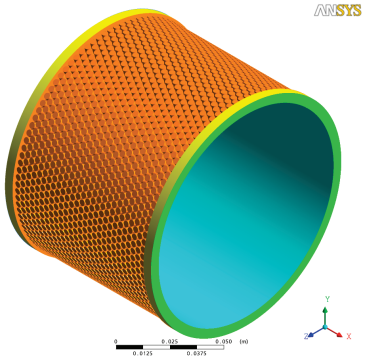

Fig. 2 Hole-pattern seal specification and parameters (left) & fluid structure (right). From (Nielsen et al., 2012)

stiffness and damping coefficients are shown in Fig. 3 & 4 and are found using CFD, ISOTSEAL and experimental work originating from Turbolab (Nielsen et al., 2012; Dawson et al., 2002). The estimated model uncertainty between the CFD and experimental results is marked as the grey area in the figures, and this information is utilized when synthesizing robust controllers. In the case of using ISOTSEAL as a nominal seal model, larger uncertainties must be expected and hence included in the uncertainty model.

3. Robust Control Design

In this section a robust controller is designed using μ synthesis to handle realistic uncertainties and changes in the seal dynamics. This controller is compared to a $\mathcal{H}_\infty$ controller based on nominal system model.

3.1. Control Design Objectives and Challenges

- Due to model uncertainties and changes in operational conditions, the controller should deliver robust performance to plants with seal stiffness and damping coefficients within ±40 % of the nominal values. Mass coefficients are neglected since the fluid is air (Nielsen et al., 2012).
- The system should be robust against other unmodelled dynamics and against system changes over time due to

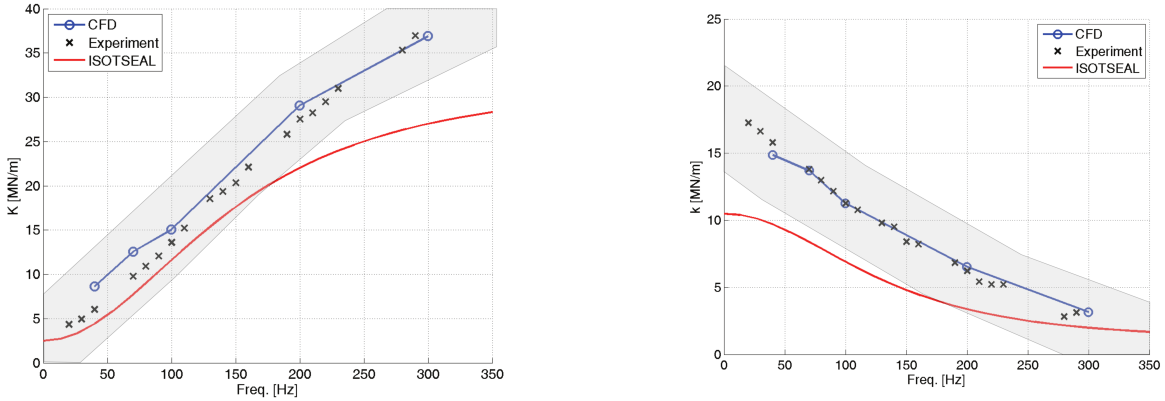

Fig. 3 Hole-pattern seal direct and cross coupled stiffness coefficients obtained using CFD, Experiment and ISOTSEAL. Figures adapted from (Nielsen et al., 2012)

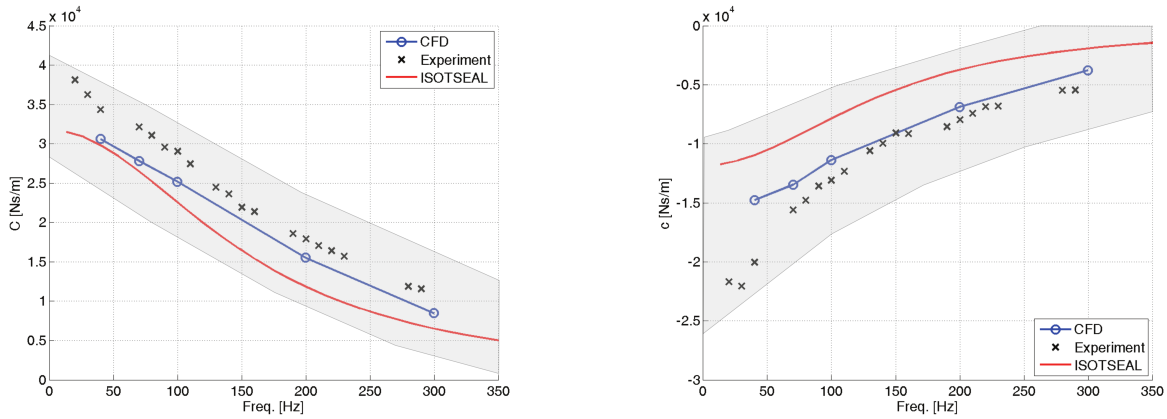

Fig. 4 Hole-pattern seal direct and cross coupled damping coefficients obtained using CFD, Experiment and ISOTSEAL. Figure adapted from (Nielsen et al., 2012)

wear and ageing. These robustness criteria are specified in ISO 14839-3, which states that the closed loop sensitivity (disturbance to error) should be less than 3 for all frequencies in order to be classified as Zone A (ISO 14839-3, 2006).

- Unbalance response should be less than 100 μm for the complete operating range, assuming the shaft is balanced according to the G2.5 standard.
- The control currents should stay well within the actuation limits of ±5 A.
- Settling time should be less than 20 ms for step disturbances on input (force) and output (displacement).

3.2. Uncertainty Representation

The nominal rotordynamic model consists of the reduced order shaft model, the negative stiffness from the AMBs and the nominal stiffness and damping from the seals. The perturbation model G_{fi} is constructed using the nominal model and the uncertainty representation, which are combined and written in LFT form. Here Δ is a 8×8 diagonal matrix representing the normalized uncertainties. G_{fi} can be written in state space form, as shown in Eq. (5), where A, B and C are the nominal system matrices. Here the input and output matrices are extended from the nominal model to include the input and output mapping B_Δ and C_Δ. Note that no extra system dynamics is added since the LFT only changes the nominal system matrix A.

$$G_{fi} = \left[\begin{array}{c|cc} A & B_\Delta & B \\ \hline C_\Delta & 0 & 0 \\ C & 0 & 0 \end{array}\right] \tag{5}$$

B_Δ and C_Δ are constructed as follows and a thorough description of this process can be seen in (Lauridsen et al., 2015). It can be shown that changes in stiffness (or damping) in a single direction at e.g. A_x corresponds to a change in a single

column of system matrix A, which corresponds to the node j where the stiffness (or damping) is altered.

$$A_{\Delta_f} = \begin{bmatrix} 0 & \dots & 0 & a_{1,j} & 0 & \dots & 0 \\ 0 & \dots & 0 & a_{2,j} & 0 & \dots & 0 \\ \vdots & \ddots & \vdots & \vdots & \vdots & \ddots & \vdots \\ 0 & \dots & 0 & a_{i,j} & 0 & \dots & 0 \end{bmatrix} \tag{6}$$

The change of the system matrix in reduced form A_Δ is found using the same modal truncation matrices as used to reduce the nominal system, as shown in Eq. (7). It is noted that the applicability of using the same modal truncation matrices to reduce the matrix representing the change in system dynamics – as were used for reducing the nominal system matrix – is based on assumption rather than proof, however, this assumption has been shown to hold well in practice. A_{Δ_f} in Eq. (6) can also be written as a column vector B_{Δ_f} and a row vector C_{Δ_f} and the change/uncertainty Δ. The input mapping B_Δ and output mapping C_Δ of the uncertainties are thus given as shown in Eq. (9). Repeating this process 8 times (one for each stiffness and damping parameter) and assembling the coloums of B_Δ and rows of C_Δ and making Δ an 8×8 diagonal matrix, yields the complete uncertainty representation.

$$A_\Delta = T_L \, A_{\Delta_f} \, T_R \tag{7}$$

$$= T_L B_{\Delta_f} \, \Delta \, C_{\Delta_f} T_R \tag{8}$$

$$= B_\Delta \, \Delta \, C_\Delta \tag{9}$$

3.3. Robust Control Design Interconnection and Weight Functions

The interconnection in Fig. 5 is used for robust controller synthesis, This is similar to the structure suggested in (Balini et al., 2012). W_p shapes the sensitivity functions i.e. the relationship from input and output disturbances W_1 and W_2 to the displacement error e. The inverse of W_p is shown in Fig. 6 and the weighting function has multiple purposes: I) Set a low sensitivity at low frequencies to obtain an integral effect, which eliminates steady state error in position reference. II) it has an upper limit of 3 which limits the maximum peak of the sensitivity functions for robustness. III) The crossover frequency indicates the bandwidth of the closed loop system (Skogestad & Postlethwaite, 2007). To achieve a settling time from disturbances of 20 ms the crossover frequency is set to 50 Hz. The weight W_u is a high-pass filter with a crossover frequency at 1.3 kHz which limits the bandwidth and amplitude of the control action.

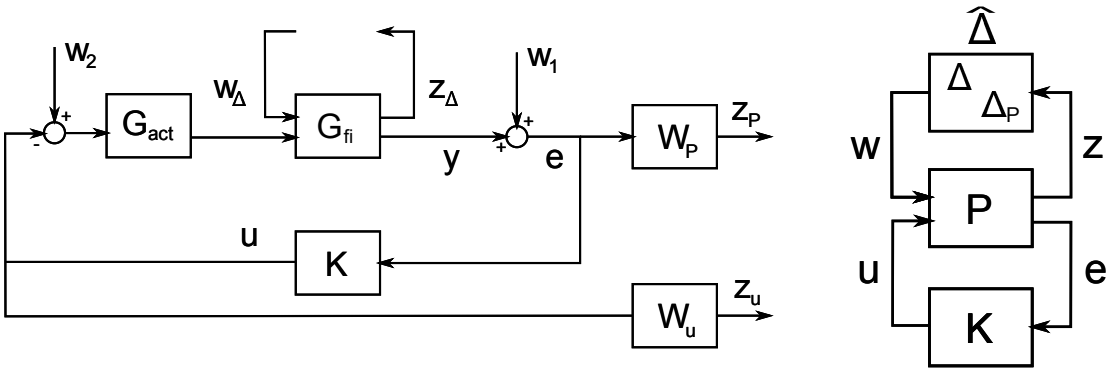

Fig. 5 Left figure: Interconnection of actuator model G_{act}, rotordynamic model with uncertainty representation G_{fi}, performance weight functions W_P and W_u, and controller K. Right figure: interconnection rearranged augmented system rearranged to the augmented system P externally connected to the controller and $\hat{\Delta}$ containing Δ for uncertain plant representation and Δ_P as full complex perturbation for performance specification.

3.4. Robust Control Synthesis

Fig. 5 (right) shows the interconnection rearranged for controller synthesis such that P is the fixed augmented plant. Note that Δ for uncertain plant representation and Δ_P (full perturbation matrix representing the $\mathcal{H}_\infty$ performance specification) are collected into the diagonal elements of $\hat{\Delta}$. Hence synthesising a controller can be done by finding a controller that minimises the ∞ norm of the transfer function from w to z, formulated as a lower LFT

$$\gamma = \|F_l(P, K)\|_\infty \tag{10}$$

The uncertainty is scaled to 1, meaning that robust performance is meet when γ is below 1. γ larger than 1 means that either the uncertainty, the performance weights or both should be scaled by $\frac{1}{\gamma}$ for the solution to hold. Solving Eq. (10) using $\mathcal{H}_\infty$ synthesis resulted in a $\mathcal{H}_\infty$ controller with γ of 618. Since this is far above 1, this controller does not guarantee robust performance.

3.4.1. Reduce Conservatism by D-scaling Using $\mathcal{H}_\infty$ directly on the problem in Fig. 5 (right) is known to suffer from conservatism since the $\hat{\Delta}$ would be considered to be a full order complex perturbation. This is commonly solved using DK-iteration, where a scaling matrix D is found, scaling w and z by D and D^{-1} to reduce the conservatism. The D matrix is found using μ synthesis in MATLAB which results in a performance index of 1.1, meaning that the system nearly guarantees robust performance.

3.5. Results

The input and output closed loop sensitivity functions, S_i and S_o, with parameter variations of ±40 % relative to nominal plant are shown in Fig. 6 (left) using an $\mathcal{H}_\infty$ controller based on a nominal plant and is shown in Fig. 6 (right) using μ synthesized controller based on the uncertain plant representation. The sensitivity peak is above 10 dB using the $\mathcal{H}_\infty$ controller based on nominal plant, and thus does not meet the requirements. Fig. 7 and Fig. 8 shows the displacement

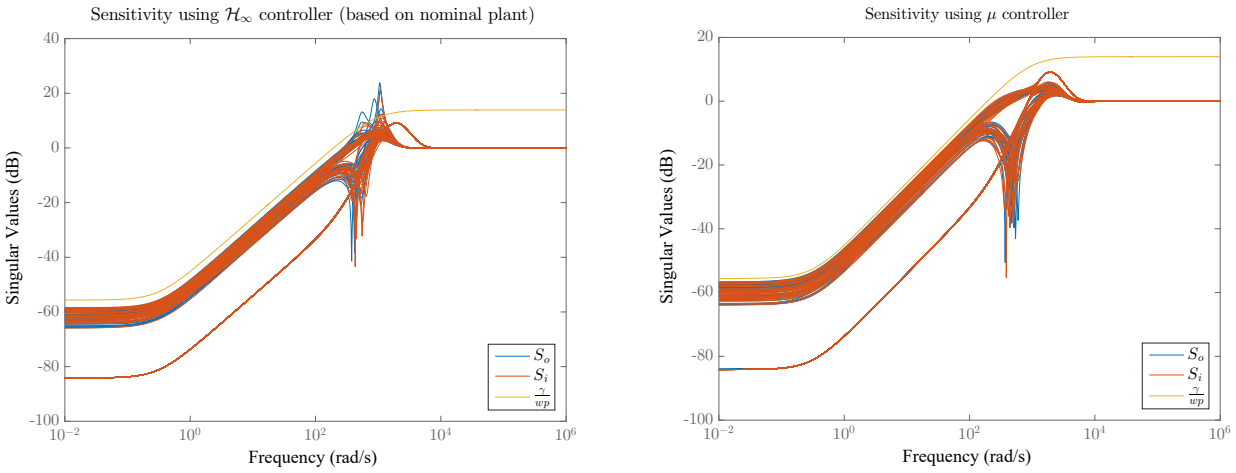

Fig. 6 Closed-loop sensitivity using $\mathcal{H}_\infty$ synthesized controller based on nominal plant (left) and using μ synthesized controller based on perturbation plant (right)

and control currents of an impulse response of the closed loop system. Nodes A_x, A_y, B_x and B_y are the locations of AMB A and B. The impulse disturbance has an amplitude of 100 N and length of 2 ms and enters through node A_x. Multiple simulations are shown for different parameter variations within ±40 %. It is clearly seen that the μ controller delivers consistent robust performance, whereas the $\mathcal{H}_\infty$ controller does not, even turning unstable for some parameter variations. It is observed that although the system is disturbed in x-direction, there is also movement in y-direction due to cross-coupling from the seal and gyroscopic forces. An unbalance simulation response according to the G2.5 standard, using the μ controller, shows that control current stays below 0.5 A and displacement stays within 25 μm for ±40 % parameter variations and thus meets the requirements. The results are though omitted in this work.

4. LPV Control Design

A Linear Parameter Varying (LPV) controller is synthesized using the Linear Matrix Inequality (LMI) formulation from (Apkarian & Adams, 1998) and using the control interconnection and weighting functions shown in Fig. 5. However, instead of using the perturbed plant representation G_{fi}, a LPV plant is used for control synthesis and simulation. For this case study it is assumed that the coefficients for the hole pattern seal over the excitation frequency range of 20-300 Hz represents the synchronous coefficients for the rotational speed range of 20-300 Hz.

4.1. Results of Spin-up Test - LPV vs μ Controller

A spin-up simulation response, demonstrating the performance of the LPV and μ controller over the operating range of 20-300 Hz with a duration of 1 s, is carried out. Step disturbances are applied every 50 ms, alternating between acting on the input and output signals. A force input disturbance of 100 N enters after 0.70 s and a displacement output disturbance

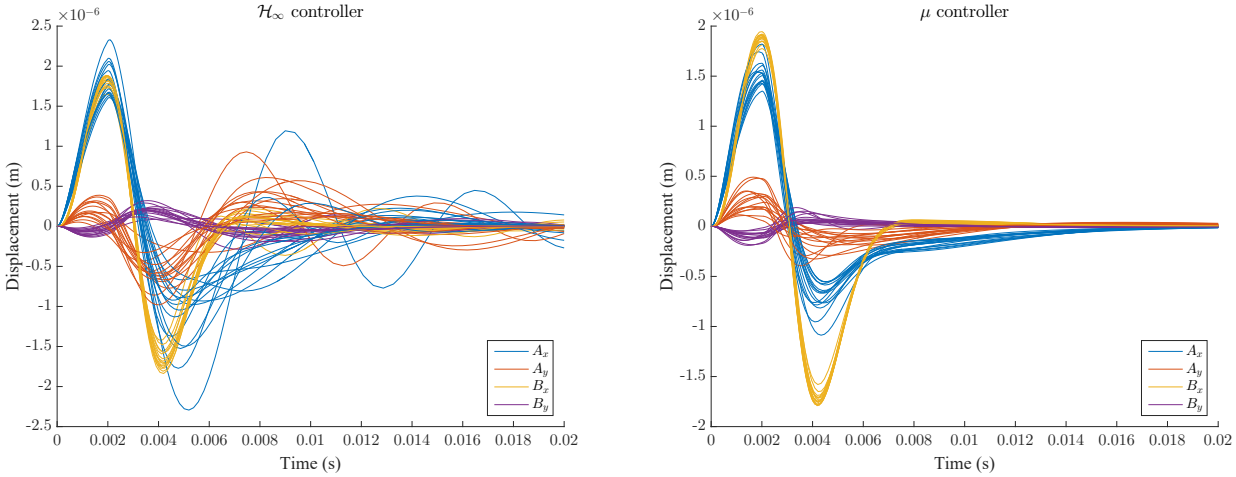

Fig. 7 Impulse response using $\mathcal{H}_\infty$ synthesized controller based on nominal plant (left) and using μ synthesized controller based on perturbation plant (right)

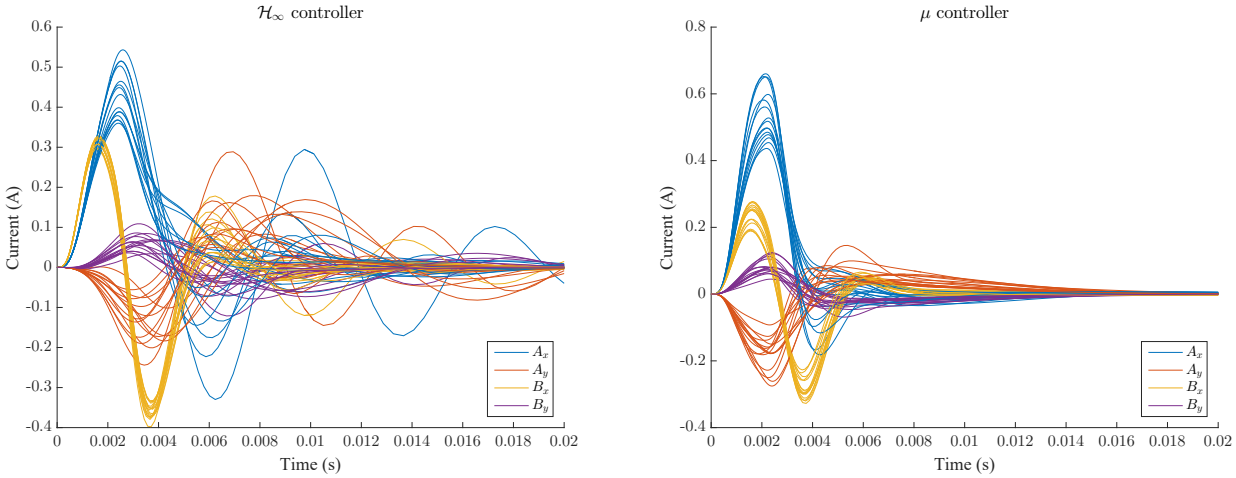

Fig. 8 Control action in response to an impulse disturbance using $\mathcal{H}_\infty$ synthesized controller based on nominal plant (left) and using μ synthesized controller based on perturbation plant (right)

of 2 μm enters after 0.75 s, both at A_x. An enlargement of a section of the response is shown in Fig. 9 (left). It is observed, that for this operational range, the LPV controller has a faster settling time, below 20 ms as required, where the μ controller takes longer time. The response is more oscillatory in the case of the μ synthesized controller compated to the LPV controller.

Fig. 9 (right) shows S_o using LPV and μ controllers for plant variations due to plant changes in the operational speed range of 20-300 Hz. The plot confirms worse performance of the μ synthesized controller, i.e: I) Oscillatory behaviour due to higher peak of S_o. II) Slower disturbance rejection due to lower crossover frequency.

5. Conclusion

Robust control design is suggested for handling uncertain seal forces in AMB systems. Significant performance improvement is shown for robust control, incorporating uncertainty model, compared to nominal model based control. This clearly demonstrates the need for incorporating uncertainties into the model based controller design process to obtain robust performance. In the case of significant frequency dependence of the dynamic seal characteristic, as for the hole pattern seal, combined with large variations in operational speed, it is hard, if not infeasible, to design a single robust LTI controller that provides satisfactory performance over the complete operational range. This paper demonstrates the performance improvement a LPV controller can deliver, compared to a single robust LTI controller. Future work will provide experimental verification of the results presented here, including testing of uncertain and changing seal forces using the test facility presented in (Voigt et al., 2016).

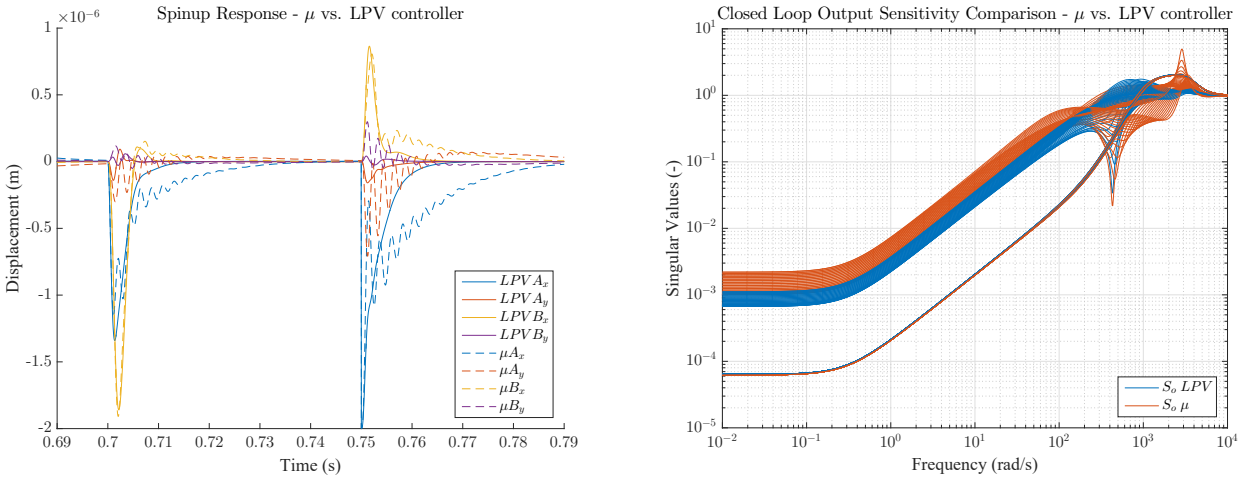

Fig. 9 Left: Spin-up test time response comparison, using LPV and μ controllers. A force input disturbance of 100 N enters after 0.70 s and a displacement output disturbance of 2 μm enters after 0.75 s, both at A_x. Right: Closed loop output sensitivity using LPV and μ controllers for plant variations due to change in operational speed in the range 20-300 Hz.

References

Lang, O., J. Wassermann, and H. Springer. "Adaptive vibration control of a rigid rotor supported by active magnetic bearings." Journal of engineering for gas turbines and power 118.4 (1996): 825-829.

Mushi, S. E., Z. Lin, P. Allaire and S. Evans "Aerodynamic cross-coupling in a flexible rotor: Control design and implementation." Proceedings of the 1 hh International Symposium on Magnetic Bearings. Nara, Japan. 2008.

Pesch, A. H., and J. T. Sawicki. "Stabilizing Hydrodynamic Bearing Oil Whip With -Synthesis Control of an Active Magnetic Bearing." ASME Turbo Expo 2015: Turbine Technical Conference and Exposition. American Society of Mechanical Engineers, 2015.

Nielsen, K. K., K. Joenck, and H. Underbakke. "Hole-Pattern and Honeycomb Seal Rotordynamic Forces: Validation of CFD-Based Prediction Techniques." Journal of Engineering for Gas Turbines and Power 134.12 (2012): 122505.

Nelson, H. D. "A finite rotating shaft element using Timoshenko beam theory." Journal of mechanical design 102.4 (1980): 793-803.

Dawson, M., D. Childs, C. Holt, S. Phillips. "Theory Versus Experiments for the Dynamic Impedances of Annular Gas Seals: Part 2Smooth and Honeycomb Seals." ASME J. Eng. Gas Turbines Power 24 (2002): 963-970.

Schonhoff, U., J. Luo, G. Li, E. Hilton, R. Nordmann. "Implementation results of mu-synthesis control for an energy storage flywheel test rig." The Eight International Symposium on Magnetic Bearings ISMB-8, Zurich, Switzerland. 2000.

Balas, G. J., and P. M. Young. "Control design for variations in structural natural frequencies." Journal of Guidance, Control, and Dynamics 18.2 (1995): 325-332.

ISO 14839-3, Vibration of rotating machinery equipped with active magnetic bearings Part 3: Evaluation of stability margin, International Standards Organization, 2006.

Balini, H. M. N. K., J. Witte, and C. W. Scherer. "Synthesis and implementation of gain-scheduling and LPV controllers for an AMB system." Automatica 48.3 (2012): 521-527.

Skogestad, S., and I. Postlethwaite. Multivariable feedback control: analysis and design. Vol. 2. New York: Wiley, 2007.

Lauridsen, J. S., A. K. Sekunda, I. F. Santos, and H. Niemann. "Identifying parameters in active magnetic bearing system using LFT formulation and Youla factorization." Control Applications (CCA), 2015 IEEE Conference on. IEEE, 2015.

Apkarian, P., and R. J. Adams. "Advanced gain-scheduling techniques for uncertain systems." Control Systems Technology, IEEE Transactions on 6.1 (1998): 21-32.

Voigt, A. J., K. Nielsen, and I. F. Santos. "Design and Calibration of a Full Scale Active Magnetic Bearing Based Testing Facility for Investigating Rotordynamic Properties of Turbomachinery Seals in Multiphase Flow". Proceedings of the ASME Turbo Expo 2016.